Raster mode continuous-flow liquid microjunction mass spectrometry imaging of proteins in thin tissue sections

Griffiths, Rian; Randall, Elizabeth; Race, Alan; Bunch, Josephine; Cooper, Helen

DOI:
10.1021/acs.analchem.7b00977

Document Version
Publisher's PDF, also known as Version of record

Citation for published version (Harvard):
Griffiths, R, Randall, E, Race, A, Bunch, J & Cooper, H 2017, 'Raster mode continuous-flow liquid microjunction mass spectrometry imaging of proteins in thin tissue sections', *Analytical Chemistry*, vol. 89, no. 11, pp. 5683–5687. https://doi.org/10.1021/acs.analchem.7b00977

analytical chemistry

Letter

pubs.acs.org/ac

Raster-Mode Continuous-Flow Liquid Microjunction Mass Spectrometry Imaging of Proteins in Thin Tissue Sections

Rian L. Griffiths,[†,#] Elizabeth C. Randall,[†,‡,#] Alan M. Race,[§,#] Josephine Bunch,[*,§,∥] and Helen J. Cooper[*,†]

[†]School of Biosciences, University of Birmingham, Edgbaston, Birmingham B15 2TT, U.K.

[‡]PSIBS Doctoral Training Centre, University of Birmingham, Edgbaston, Birmingham B15 2TT, U.K.

[§]National Physical Laboratory, Hampton Road, Teddington, Middlesex TW11 0LW, U.K.

[∥]School of Pharmacy, University of Nottingham, University Park, Nottingham NG7 2RD, U.K.

Supporting Information

ABSTRACT: Mass spectrometry imaging by use of continuous-flow liquid microjunction sampling at discrete locations (array mode) has previously been demonstrated. In this Letter, we demonstrate continuous-flow liquid microjunction mass spectrometry imaging of proteins from thin tissue sections in raster mode and discuss advantages (a 10-fold reduction in analysis time) and challenges (suitable solvent systems, data interpretation) of the approach. Visualization of data is nontrivial, requiring correlation of solvent-flow, mass spectral data acquisition rate, data quality, and liquid microjunction sampling area. The latter is particularly important for determining optimum pixel size. The minimum achievable pixel size is related to the scan time of the instrument used. Here we show a minimum achievable pixel size of 50 μm (x-dimension) when using an Orbitrap Elite; however a pixel size of 600 μm is recommended in order to minimize the effects of oversampling on image accuracy.

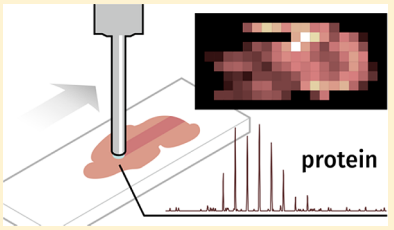

Liquid microjunction (LMJ) sampling of surfaces may be performed either by use of predetermined discrete volumes of solvent or by use of a continuous flow of solvent. The former was first described by Kertesz and Van Berkel[1] and has become known as liquid extraction surface analysis (LESA). LESA has been shown to be suitable for the analysis of small molecules such as drugs and their metabolites,[2,3] lipids,[4,5] intact proteins,[6−9] and protein assemblies[10−12] from a range of substrates including thin tissue sections, bacterial colonies, and dried blood spots. Recently, we described intact protein imaging via LESA mass spectrometry.[13] The continuous-flow approach was first demonstrated for the analysis of small molecule dyes from thin layer chromatography plates, also by Van Berkel and co-workers,[14] and is now available commercially as the Flowprobe platform. Continuous-flow LMJ sampling via the Flowprobe has been applied to the analysis of metabolites from bacteria and fungi[15] and drugs in dried blood spots.[16]

Mass spectrometry imaging by use of the Flowprobe has been demonstrated for the antibiotic levofloxacin in rabbit lung tissue,[17] metabolites in liver, brain, and lung tissues[18] and proteins in rat kidney,[19] rat brain, and human ovarian tissue.[20] In each case, imaging was performed in array mode. That is, discrete locations are probed by continuous-flow LMJ sampling and after each sampling event the probe is raised and flushed before moving to the next discrete location, and the process is repeated for the full array. A potential advantage of the Flowprobe is that it can be operated in raster mode, in which the sample stage below the probe is moved at a constant speed while the liquid microjunction is maintained. This mode of operation has been demonstrated in Flowprobe analysis of lipids from cytospins prepared from a breast cancer cell line,[21] although in that study the rationale for rastering was complete extraction of the cells rather than spatial profiling. Raster-mode ion imaging offers potential benefits in terms of both throughput and reduced pixel size. Laskin and co-workers have demonstrated raster imaging of a range of analytes by nano-DESI, a variant of continuous-flow liquid microjunction sampling.[22,23] Hsu et al.[24] recently demonstrated raster-mode imaging of proteins in thin tissue sections using a home-built nano-DESI source, achieving pixel sizes of 40 μm.

Here, we demonstrate continuous-flow liquid microjunction mass spectrometry imaging, by use of the commercially available Flowprobe, of proteins from thin tissue sections in raster mode. Visualization and quality of image data are discussed.

METHODS

Samples. Brain from wild-type mice (extraneous tissue from culled animals) were the gift of Prof. Steve Watson (University of Birmingham). Organs were frozen on dry ice prior to storage at −80 °C. Sagittal sections of mouse brain tissue of area ∼1.5 cm^2 were obtained at a thickness of 10 μm using a CM1810

Received: March 16, 2017
Accepted: May 11, 2017
Published: May 11, 2017

DOI: 10.1021/acs.analchem.7b00977
Anal. Chem. 2017, 89, 5683−5687

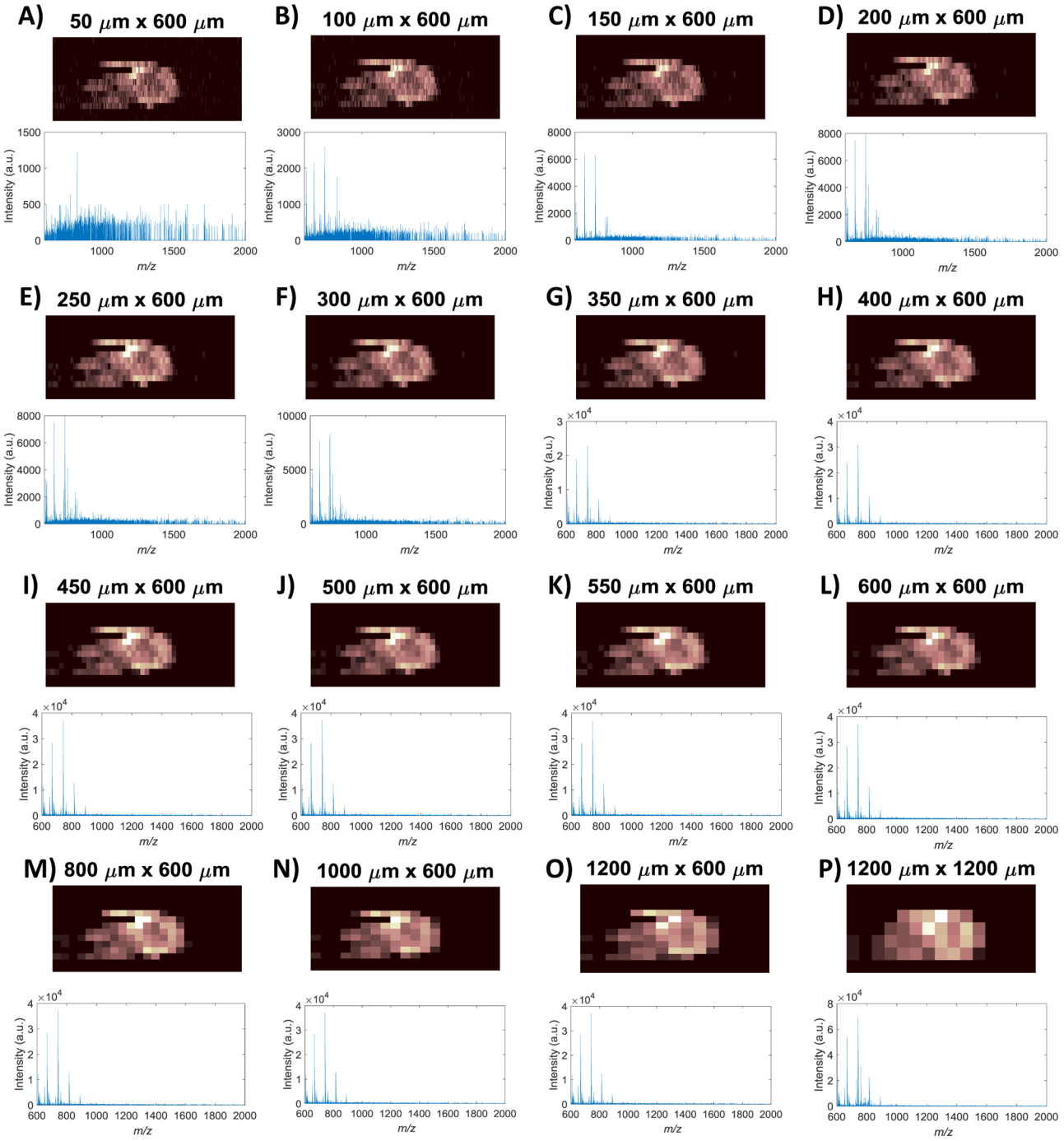

Figure 1. Raster-mode Flowprobe mass spectrometry imaging of mouse brain. Panels A–O, ion images of β thymosin 4 (m/z 828^{6+}; MW 4961 Da) are shown at 600 μm (y dimension, relating to the line spacing) and at increasing pixel sizes (x dimension) from 50 to 1200 μm, corresponding to the distance traveled to acquire (A) a single scan mass spectrum (50 μm), (B) 2-co-added mass spectra (100 μm), up to (O) 24 coadded spectra (1200 μm). Representative single pixel mass spectra are shown alongside each ion image. Panel P, ion image plotted at 1200 μm (x dimension) × 1200 μm (y dimension) corresponding to a total of 48 coadded spectra in a single pixel mass spectrum.

Cryostat (Leica Microsystmes, Wetzlar, Germany) and thaw mounted onto glass slides.

Flowprobe MSI. Mass spectrometry imaging was performed by use of the Flowprobe (Prosolia, Indiana, Indianapolis). Tissue samples were scanned with an Epson scanner and the JPEG image was loaded into the Flowprobe nMotion software. Tissue sample slides were mounted into the Flowprobe stage. The nMotion software was operated in rastering mode for imaging. For all experiments, 50:50 MeOH–H_2O with 1% formic acid was used as the extraction solvent and the inner capillary was retracted ~100 μm relative to the probe tip. The solvent delivery flow rate was 10 μL/min. The sample stage was rastered at a speed of 80 μm/s under the probe, with 600 μm spacing between raster lines. The Flowprobe was coupled with an Orbitrap Elite mass spectrometer (Thermo Fisher Scientific, Bremen, Germany). Mass spectra were recorded in full scan mode (m/z 600–2000) at a resolution of 120 000 at m/z 400. Automatic gain control

DOI: 10.1021/acs.analchem.7b00977
Anal. Chem. 2017, 89, 5683–5687

(AGC) was turned off for imaging experiments. The fill time (200 ms) to accumulate 1×10^6 charges was optimized prior to analysis.

Data Analysis. Raster mode imaging data were converted to mzML format using msconvert as part of ProteoWizard[25] and then to the imzML format using imzMLConverter.[26] Data in imzML format were then loaded into MATLAB (version 2013a, The MathWorks Inc., Natick, Massachusetts) using imzMLConverter and SpectralAnalysis software.[27] Ion images were displayed with aspect ratios which reflect the size of the sampled area within each pixel, assuming no oversampling. For raw data that equates to 50 μm (x dimension, based on the scan time of 0.63 s and a stage speed of 80 μm/s) by 600 μm (y dimension, based on distance between raster lines). To simulate larger pixel sizes, sequential scans were summed and displayed with an aspect ratio corresponding to the new pixel dimensions.

RESULTS

Previous work in our laboratory has shown that the optimum solvent systems for liquid microjunction sampling of proteins from tissue are aqueous acetonitrile solutions;[8,28] however, such solvent systems present a challenge for the Flowprobe. The Flowprobe capillary is coated with polyimide which swells in the presence of acetonitrile[29] with obvious consequences for maintenance of the liquid microjunction. A 10 μL/min flow of 50% acetonitrile resulted in extension of the capillary of ~130 μm after 30 min (see Supplemental Figure 1). While that occurrence could in principle be managed in array mode imaging by regularly exchanging the capillary, albeit with a significant cost, that approach is not feasible in raster mode. Consequently, an alternative solvent system comprising 50% methanol (and 1% formic acid) was used.

Raster sampling of a sagittal section of mouse brain was performed at a raster speed of 80 μm/s, the slowest speed available with this system. The diameter of the Flowprobe tip is ~600 μm, and therefore the spacing between raster lines was 600 μm. A total of 14 raster lines (length = 17 mm) were acquired. The total analysis time was therefore 57 min 41 s (3 min 32 s per line plus 35 s flushing between lines). That compares favorably with the time required to acquire an image in array mode. An equivalent area 600 μm array (28 by 14, total of 392 sample spots) would require ~10 h analysis time, assuming 1 min sampling followed by 35 s system flushing at each location. (Note that while higher raster speeds would naturally reduce analysis time, the corollary would be an increase in minimum achievable pixel size, see below).

Table 1. Percentage of the Total Sampled Region Which Is Outside of the Visualized "Pixel" (Assumes a Circular Liquid Microjunction with Diameter 600 μm)

pixel size	percentage of total sampled area outside of "pixel"
50 × 600	90.4
100 × 600	82.5
150 × 600	75.9
200 × 600	70.2
250 × 600	65.3
300 × 600	61.1
350 × 600	57.4
400 × 600	54.1
450 × 600	51.1
500 × 600	48.5
550 × 600	46.1
600 × 600	44.0

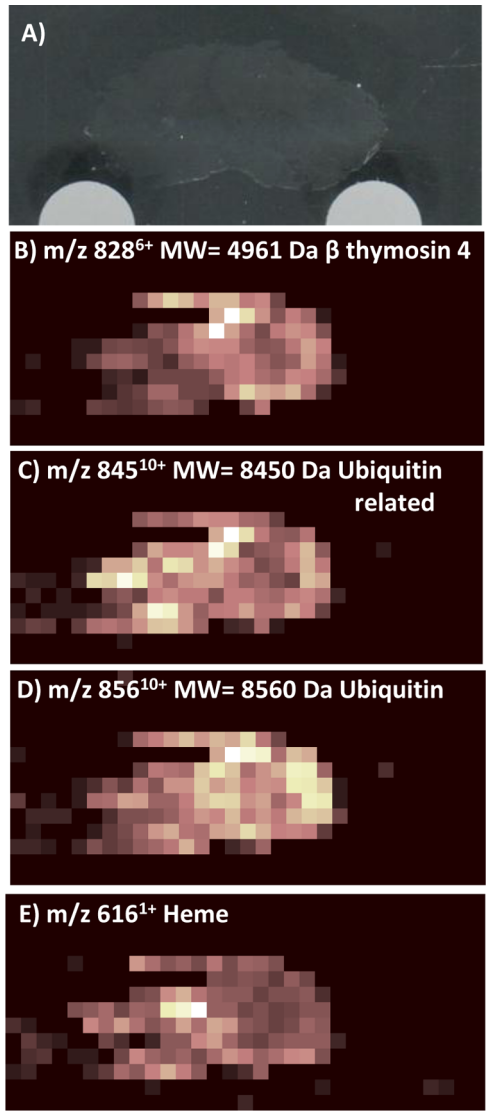

Figure 2. Raster-mode Flowprobe mass spectrometry imaging of mouse brain. Photograph of the mouse brain tissue section (A) and ion images of (B) β thymosin 4; (C) truncated ubiquitin (Ub-GG); (D) ubiquitin and (E) heme at pixel size 600 × 600 μm.

There are a number of factors that must be taken into consideration when visualizing raster-mode imaging data acquired by continuous-flow liquid microjunction sampling. First, the time for analytes to travel from the surface through the capillary to the electrospray source must be taken into account. The volume of the capillary is 5.035 μL; therefore, at a solvent flow rate of 10 μL/min, signal is detected after 30 s. Second, the rate of mass spectral data acquisition must be considered. To illustrate, if the mass spectrum takes 2 s to acquire and the raster speed was 100 μm/s, the minimum pixel size (regardless of data quality) would be 200 μm. In our experiments, single scan spectra were acquired in 0.63 s, and therefore, at a raster speed of 80 μm/s, the minimum pixel size was 50 μm in the x dimension. (Recall that the spacing between raster lines was 600 μm; hence, the pixel size in the y dimension remains constant at 600 μm). Coupling the Flowprobe to a mass spectrometer capable of acquiring data with shorter scan

DOI: 10.1021/acs.analchem.7b00977
Anal. Chem. 2017, 89, 5683−5687

times, such as a TOF, QTOF, or QQQ instrument, would enable even smaller minimum pixel sizes. It is common practice to improve data quality (S/N) by coadding multiple scans. The consequence of this practice for raster mode imaging is increasing pixel size. Co-addition of two mass spectra increase the pixel size (x dimension) to 100 μm, three coadded mass spectra give a pixel size of 150 μm and so on. Figure 1 shows ion images for the 6+ charge state of β-thymosin 4 (m/z 828) visualized at a range of pixel sizes. (Note that for the second on-tissue raster line, the liquid microjunction failed approximately half way across and no signal was observed for the latter part of the raster. Raster scans from right to left across tissue). The pixel size in panel A is 50 μm × 600 μm, representing single scan mass spectra. In panel B, individual pixels correspond to two coadded spectra. The lower section of each panel shows representative single pixel mass spectra. As the pixel size increases, i.e., more mass spectra are coadded, the spectral quality (S/N) improves, as expected; however, peaks are detected even in the single scan mass spectra indicating that data quality is not the limiting factor in determining minimum pixel size.

The above comments focus on achievable pixel size based solely on the correlation of raster speed and mass spectral acquisition speed; however, a key issue is the liquid microjunction sampling area (~600 μm diameter). Continuous-flow liquid microjunction sampling of a single location on tissue gives a protein signal in the mass spectrum for a minimum of 3 min (data not shown). The time taken for the liquid microjunction to pass a distance of 600 μm (i.e., the diameter of the liquid microjunction) at a raster speed of 80 μm/s is 7.5 s. That is, analytes from the tissue at the trailing edge of the liquid microjunction are being extracted simultaneously to those being extracted from fresh tissue at the leading edge of the microjunction. Regardless of given pixel size, the signal displayed for a particular pixel could have derived from any location within the preceding 600 μm of the raster. Table 1 shows the percentage of the total sampled area (A_s) which falls outside of the visualized pixel (A_v), see Supplemental Figure 2.

$$\% = 100 - \left(\frac{A_v}{A_s}\right)$$

where A_s = [area of liquid microjunction (πr^2, r = 300 μm) + A_v].

Depending on the pixel size used to reconstruct the data, the percentage of the sampled area which falls outside of the visualized "pixel" area could be as high as 90.4%, meaning the visualized pixel represents just 9.6% of the area that was actually sampled. This feature has similar implications in other MSI techniques which employ raster mode, such as DESI, nano-DESI and, to a lesser extent, MALDI (if the matrix is not fully ablated within a given pixel area).[30]

With the exception of the start and end of the raster line, the extent to which a tissue location has been sampled is constant, which may minimize the apparent effect on the ion images. Use of pixels of equivalent dimensions to the liquid microjunction will also minimize the effect. Use of larger pixels are demonstrated to confer no benefit in this case, see Figure 1 panels M to P. For comparison, raster mode sampling of a line of ink (width 540 μm) containing rhodamine dye on glass substrate was performed, see Supplemental Figure 3. Plots of relative intensity versus distance traveled at various pixel sizes reveal that no resolution benefit is gained at pixel sizes smaller than 300 μm. It is, however, very important to note that the two surfaces (tissue and glass) are very different in terms of surface wettability and consequently the size of the liquid microjunction is much larger for glass than tissue (see Supplemental Figure 3I). Comprehensive evaluation of the resolution and image quality achievable for Flowprobe protein imaging in tissue requires lateral resolution standards comprising tissue mimetics, which are not currently available. In their absence, the recommendation is to visualize ion images at pixel sizes equivalent to the probe area. For example, see Figure 2, which shows ion images of three proteins (β-thymosin 4, 6+ charge state, m/z 828; ubiquitin, 10+ charge state, m/z 856; C-terminal truncated ubiquitin, 10+ charge state, m/z 845) and singly charged heme ions (m/z 616) at pixel size 600 × 600 μm.

CONCLUSION

The results demonstrate that raster-mode imaging of proteins in thin tissue sections may be achieved by use of continuous-flow liquid microjunction sampling via the Flowprobe coupled with an orbitrap mass spectrometer. The S/N observed in a single scan is sufficient to allow a minimum pixel size of 50 μm (x-dimension). Nevertheless, oversampling due to the larger area of the liquid microjunction means that larger pixel sizes (e.g., 600 μm) are preferred to ensure accuracy in the images.

ASSOCIATED CONTENT

Supporting Information

The Supporting Information is available free of charge on the ACS Publications website at DOI: 10.1021/acs.analchem.7b00977.

Photograph of the inner capillary of the Flowprobe system after ~30 minutes solvent flow where solvent comprised 50% acetotrile/1% formic acid; schematic illustrating total sampled area versus visualised pixel; and raster-mode Flowprobe mass spectrometry imaging of rhodamine dye in ink (PDF)

AUTHOR INFORMATION

Corresponding Authors

*E-mail: josephine.bunch@npl.co.uk.
*E-mail: h.j.cooper@bham.ac.uk.

ORCID

Helen J. Cooper: 0000-0003-4590-9384

Author Contributions

#R.L.G., E.C.R., and A.M.R. contributed equally to this work.

Notes

The authors declare no competing financial interest.

Supplementary data supporting this research is openly available from the University of Birmingham data archive at http://findit.bham.ac.uk/.

ACKNOWLEDGMENTS

H.J.C. and R.L.G. are funded by EPSRC (EP/L023490/1). E.C.R. received funding from the EPSRC via the PSIBS Doctoral Training Centre (EP/F50053X/1), in collaboration with Astra Zeneca and the National Physical Laboratory. A.M.R. and J.B. gratefully acknowledge funding through the NPL Strategic Research Project AIMS HIGHER (Grant 119375). The Thermo Fisher Orbitrap Elite mass spectrometer

DOI: 10.1021/acs.analchem.7b00977
Anal. Chem. 2017, 89, 5683−5687

used in this research was funded through Birmingham Science City Translational Medicine, Experimental Medicine Network of Excellence Project with support from Advantage West Midlands. The authors thank Klaudia Kocurek for creation of the TOC graphic.

REFERENCES

(1) Kertesz, V.; Van Berkel, G. J. *J. Mass Spectrom.* **2010**, *45*, 252−260.
(2) Eikel, D.; Vavrek, M.; Smith, S.; Bason, C.; Yeh, S.; Korfmacher, W. A.; Henion, J. D. *Rapid Commun. Mass Spectrom.* **2011**, *25*, 3587−3596.
(3) Swales, J. G.; Tucker, J. W.; Strittmatter, N.; Nilsson, A.; Cobice, D.; Clench, M. R.; Mackay, C. L.; Andren, P. E.; Takáts, Z.; Webborn, P. J.; Goodwin, R. J. A. *Anal. Chem.* **2014**, *86*, 8473−8480.
(4) Brown, S. H.; Huxtable, L. H.; Willcox, M. D.; Blanksby, S. J.; Mitchell, T. W. *Analyst* **2013**, *138*, 1316−1320.
(5) Griffiths, R. L.; Sarsby, J.; Guggenheim, E. J.; Race, A. M.; Steven, R. T.; Fear, J.; Lalor, P. F.; Bunch, J. *Anal. Chem.* **2013**, *85*, 7146−7153.
(6) Edwards, R. L.; Creese, A. J.; Baumert, M.; Griffiths, P.; Bunch, J.; Cooper, H. J. *Anal. Chem.* **2011**, *83*, 2265−2270.
(7) Edwards, R. L.; Griffiths, P.; Bunch, J.; Cooper, H. J. *J. Am. Soc. Mass Spectrom.* **2012**, *23*, 1921−1930.
(8) Sarsby, J.; Martin, N. J.; Lalor, P. F.; Bunch, J.; Cooper, H. J. *J. Am. Soc. Mass Spectrom.* **2014**, *25*, 1953−1961.
(9) Sarsby, J.; Griffiths, R. L.; Race, A. M.; Bunch, J.; Randall, E. C.; Creese, A. J.; Cooper, H. J. *Anal. Chem.* **2015**, *87*, 6794−6800.
(10) Martin, N. J.; Griffiths, R. L.; Edwards, R. L.; Cooper, H. J. *J. Am. Soc. Mass Spectrom.* **2015**, *26*, 1320−1327.
(11) Griffiths, R. L.; Cooper, H. J. *Anal. Chem.* **2016**, *88*, 606−609.
(12) Mikhailov, V. A.; Griffiths, R. L.; Cooper, H. J. *Int. J. Mass Spectrom.* **2016**, DOI: 10.1016/j.ijms.2016.09.011.
(13) Griffiths, R. L.; Creese, A. J.; Race, A. M.; Bunch, J.; Cooper, H. J. *Anal. Chem.* **2016**, *88*, 6758−6766.
(14) Van Berkel, G. J.; Sanchez, A. D.; Quirke, J. M. E. *Anal. Chem.* **2002**, *74*, 6216−6223.
(15) Hsu, C.-C.; ElNaggar, M. S.; Peng, Y.; Fang, J.; Sanchez, L. M.; Mascuch, S. J.; Moller, K. A.; Alazzeh, E. K.; Pikula, J.; Quinn, R. A.; Zeng, Y.; Wolfe, B. E.; Dutton, R. J.; Gerwick, L.; Zhang, L.; Liu, X.; Mansson, M.; Dorrestein, P. C. *Anal. Chem.* **2013**, *85*, 7014−7018.
(16) Gaissmaier, T.; Siebenhaar, M.; Todorova, V.; Hullen, V.; Hopf, C. *Analyst* **2016**, *141*, 892−901.
(17) Prideaux, B.; ElNaggar, M. S.; Zimmerman, M.; Wiseman, J. M.; Li, X.; Dartois, V. *Int. J. Mass Spectrom.* **2015**, *377*, 699−708.
(18) ElNaggar, M. S.; Prideaux, B.; Dartois, V.; Wiseman, J. M. *Curr. Metabolomics* **2014**, *2*, 122−131.
(19) Griffiths, R. L., Randall, E. C.; Cooper, H. J. Liquid microjunction sampling for the analysis of proteins from thin tissue sections. In *64th ASMS Conference on Mass Spectrometry and Allied Topics*, San Antonio, TX, June 5−9, 2016.
(20) Feider, C. L.; Elizondo, N.; Eberlin, L. S. *Anal. Chem.* **2016**, *88*, 11533−11541.
(21) Olson, M. T.; Baxi, A.; ElNaggar, M. S.; Umbricht, C.; Yergey, A. L.; Clarke, W. *J. Am. Soc. Cytopath.* **2016**, *5*, 3−8.
(22) Laskin, J.; Heath, B. S.; Roach, P. J.; Cazares, L.; Semmes, O. J. *Anal. Chem.* **2012**, *84*, 141−148.
(23) Roach, P. J.; Laskin, J.; Laskin, A. *Analyst* **2010**, *135*, 2233−2236.
(24) Hsu, C.-C.; Chou, P.-T.; Zare, R. N. *Anal. Chem.* **2015**, *87*, 11171−11175.
(25) Chambers, M. C.; Maclean, B.; Burke, R.; Amodei, D.; Ruderman, D. L.; Neumann, S.; Gatto, L.; Fischer, B.; Pratt, B.; Egertson, J.; Hoff, K.; Kessner, D.; Tasman, N.; Shulman, N.; Frewen, B.; Baker, T. A.; Brusniak, M.-Y.; Paulse, C.; Creasy, D.; Flashner, L.; Kani, K.; Moulding, C.; Seymour, S. L.; Nuwaysir, L. M.; Lefebvre, B.; Kuhlmann, F.; Roark, J.; Rainer, P.; Detlev, S.; Hemenway, T.; Huhmer, A.; Langridge, J.; Connolly, B.; Chadick, T.; Holly, K.; Eckels, J.; Deutsch, E. W.; Moritz, R. L.; Katz, J. E.; Agus, D. B.; MacCoss, M.; Tabb, D. L.; Mallick, P. *Nat. Biotechnol.* **2012**, *30*, 918−920.
(26) Race, A. M.; Styles, I. B.; Bunch, J. *J. Proteomics* **2012**, *75*, 5111−5112.
(27) Race, A. M.; Palmer, A. D.; Dexter, A. J.; Steven, R. T.; Styles, I. B.; Bunch, J. *Anal. Chem.* **2016**, *88*, 9451−9458.
(28) Sarsby, J. *Liquid microjunction surface sampling and MALDI imaging of small and large molecules in human liver disease*. Ph.D. Thesis, University of Birmingham, Birmingham, U.K., 2016.
(29) Baeuml, F.; Welsch, T. *J. Chromatogr. A* **2002**, *961*, 35−44.
(30) Steven, R. T.; Race, A. M.; Bunch, J. *J. Am. Soc. Mass Spectrom.* **2016**, *27*, 1419−1428.

DOI: 10.1021/acs.analchem.7b00977
Anal. Chem. 2017, 89, 5683−5687